TOXICOLOGICAL SCIENCES **109(1)**, 152–167 (2009)
doi:10.1093/toxsci/kfp046
Advance Access publication February 27, 2009

Pulmonary Toxicity and Fate of Agglomerated 10 and 40 nm Aluminum Oxyhydroxides following 4-Week Inhalation Exposure of Rats: Toxic Effects are Determined by Agglomerated, not Primary Particle Size

Jürgen Pauluhn[1]

Institute of Toxicology, Bayer Schering Pharmaceuticals, 42096 Wuppertal, Germany

Received February 16, 2009; accepted February 20, 2009

Inhaled polydisperse micronsized agglomerated particulates composed of nanosized primary particles may exert their pulmonary toxicity in either form, depending on whether these tightly associated structures are disintegrated within the biological system or not. This hypothesis was tested in a rat bioassay using two calcined aluminum oxyhydroxides (AlOOH) consisting of primary particles in the range of 10–40 nm. Male Wistar rats were nose-only exposed to 0.4, 3, and 28 mg/m^3 in two 4-week (6 h/day, 5 days/week) inhalation studies followed by a 3-month post-exposure period. The respective mass median aerodynamic diameter (MMAD) of agglomerated particles in inhalation chambers was 1.7 and 0.6 μm. At serial sacrifices, pulmonary toxicity was characterized by bronchoalveolar lavage (BAL) and histopathology. The retention kinetics of aluminum (Al) was determined in lung tissue, BAL cells, and selected extrapulmonary organs, including lung-associated lymph nodes (LALNs). Significant changes in BAL, lung, and LALN weights occurred at 28 mg/m^3. Histopathology revealed alveolar macrophages with enlarged and foamy appearance, increased epithelial cells, inflammatory cells, and focal septal thickening. The determination of aluminum in lung tissue shows that the cumulative lung dose was higher following exposure to AlOOH-40 nm/MMAD-0.6 μm than to AlOOH-10 nm/MMAD-1.7 μm, despite identical exposure concentrations. The associated pulmonary inflammatory response appears to be principally dependent on the agglomerated rather than primary particle size. Despite high lung burdens, conclusively increased extrapulmonary organ burdens did not occur at any exposure concentration and postexposure time point. Particle-induced pulmonary inflammation was restricted to cumulative doses exceeding approximately 1 mg AlOOH/g lung following 4-week exposure at 28 mg/m^3. It is concluded that the pulmonary toxicity of nanosized, agglomerated AlOOH particles appears to be determined by the size of agglomerated rather than primary particles, whereas the clearance half-time of particles appears to increase with decreased primary particle size. However, in regard to toxicokinetics, this outcome is highly contingent upon the total lung burden and especially whether overloading or non-overloading conditions were attained or not. In order to reliably demonstrate retention-related different characteristics in toxicity and fate of poorly soluble (nano)particles postexposure periods of at least 3 months appear to be indispensible.

Key Words: **nanoparticles; repeated inhalation exposure; disposition; respirability; clearance; aggregates; pulmonary and extrapulmonary toxicity.**

Nanotoxicology, a subspecialty of particle toxicology, addresses the toxicology of nanoparticles (particles < 100 nm diameter) which have been claimed to have some toxic effects that are unusual and not seen with larger micronsized particles. Key studies have demonstrated with TiO_2 that ultrafine particles caused more inflammation in rat lungs than exposure to fine TiO_2 (Bermudez *et al*., 2002, 2004; Ferin *et al*., 1992). These differences in toxic potencies seem to be a result of their unique size, surface area/activity and/or crystal properties (Warheit *et al*., 2005, 2007; Warheit, 2008). In rats, pulmonary inflammatory responses increase precipitously under conditions of lung overload, a particle-induced depression of clearance as a consequence of volumetric overload of the alveolar macrophages and associated loss of alveolar macrophage mobility (Monteiller *et al*., 2007; Morrow, 1988, 1992; Stöber and McClellan, 1997). In addition, some nanoparticles seem to be able to translocate from their site of initial deposition to distant, extrapulmonary sites (Donaldson *et al*., 2006, 2008; Stern and McNeil, 2008). Dispositional end points alone only address ''internal'' exposure; however, they are considered to be important complementary data to interrelate the ''external'' exposure intensity with associated toxicodynamic effects.

Little appreciation has been given to approaches attempting to link the mere presence of particles at specific sites with associated adverse effects, including their toxicological significance. From the perspective of inhalation toxicology, it appears to be unresolved yet whether nanotoxicology has revolutionized particle toxicology and rejuvenated it or whether many of the reported characteristics that may confer toxicity are related to experimental shortcomings and especially high dose of testing strategies using noninhalational, bolus administration techniques (Maynard, 2007). The distribution and

[1] To whom correspondence should be addressed at Department of Inhalation Toxicology, Bayer Schering Pharmaceuticals, Building no. 514, 42096 Wuppertal, Germany. Fax. +49-(202)-364589. E-mail: juergen.pauluhn@bayerhealthcare.com.

biopersistence of nanoparticles, whether directly inhaled or produced by the disintegration of inhaled agglomerated nanoparticles within the lung, have received only little attention so far (DEFRA, 2007). For state-of-the-art comparison, interpretation of bioassays and risk characterization special attention needs also to be given to metrology and dosimetry aspects which means, biomarkers of effects need to be associated with markers of local dosimetry and kinetics (DEFRA, 2007; Donaldson and Seaton, 2007; Duffin *et al.*, 2007).

The purpose of the research addressed in this paper is to improve the basis for *in vivo* assessment of the toxicity of inhaled agglomerated nanoparticles by advancing the understanding of the dose-response and time-course relationships in pulmonary and extrapulmonary tissues over an exposure period of 4 weeks followed by a 3-month postexposure period. The principal hypothesis of study was to test whether the pulmonary effects (toxicity and fate) following exposure to aluminum oxyhydroxides of differing primary and agglomerated particle size are more dependent on the primary than agglomerated particle size or vice versa. Attempts are made to define the "dose in alveolar cells" and to link this endpoint with particle retention under apparent non lung-overloading and lung-overloading conditions. Such a comparison requires a mass-based metric in order to have common denominators for inhalation exposure and particle size measurements as well as tissue burdens. The model substances used were two types of aluminum oxyhydroxides (Boehmite), high-purity calcined, and agglomerated nanosized aluminas of very low solubility. These aluminas had primary isometric particles (crystals) of 10 and 40 nm. The mass median aerodynamic diameter (MMAD) of agglomerated particles in inhalation chambers was ≈1.7 and ≈0.6 μm, respectively.

The materials evaluated are free flowing high-purity agglomerated powders with optimized properties augmenting their dispersion in various systems. They found their way into a broad range of applications, including catalyst supports, coatings, polymer additives, thickeners, refractories, abrasives, ceramics as well as flame retardant in plastics. Further details regarding their use and properties are available elsewhere (http://www.sasoltechdata.com/alumina_group.asp).

METHODS

Test material. Aluminum oxyhydroxides (empirical formula: γ-AlOOH, molecular mass: 60 g/mol; Pural 200, primary particle size 40 nm; Disperal, primary particle size 10 nm; for more details see Table 1) were from Sasol (Germany). Their physical properties, such as crystalline phase, surface area, and porosity are highly controlled by calcining time and temperature (for details see (http://www.sasoltechdata.com/ alumina_group.asp). The particle size of the dispersed and nondispersed bulk AlOOH was determined by SEM (Scanning Electron Microscopy; see Fig. 1).

Animals, diet, and housing conditions. Specific pathogen free, young adult male Wistar rats of the strain Bor:WISW (SPF-Cpb) were purchased from Winkelmann (Borchen, Germany). At the commencement of the study the rats were approximately 2 months old and were quarantined for approximately 1 week prior to being used. They were singly housed in polycarbonate cages, containing low-dust wood shavings as bedding material. A standard fixed-formula diet (KLIBA 3883 = NAFAG 9441 pellets maintenance diet for rats and mice; PROVIMI KLIBA SA, 4303 Kaiseraugst, Switzerland) and municipality tap water (drinking bottles) were available *ad libitum*. The light cycle was automatically controlled in the animal room to provide 12/12-h light/darkness. Temperature and relative humidity were in the range of 22°C and 40–60%, respectively. The studies described were conducted in accordance to the EU animal welfare regulations (Directive 86/609/EEC, 1986).

TABLE 1
Physical Characteristics of Test Substances

Test substance	AlOOH-40 nm/ MMAD-0.6 μm	AlOOH-10 nm/ MMAD-1.7 μm
Commercial name:	Pural 200[a]	Disperal[a]
Empirical formula	γ-AlO(OH)	γ-AlO(OH)
Crystal structure	Boehmite (orthorhombic)	Boehmite (orthorhombic)
Aluminum content (% expressed as Al_2O_3)	82.7	77.9
Aluminum content (%)	43.9	39.4
Molecular mass (g/mol)	60	60
N_2-BET Surface area (m^2/g) at 500°C/3 h	105	182
Specific density (g/cm^3)	2.85	2.85
Loose bulk density (g/cm^3)	0.51	0.46
Pore volume (ml/g)	min. 0.7	0.5
ζ-Potential (mV) at 25°C	36	n.d.
Primary particle size (nm)	≈40	≈10
Particle size as measured on the powder—d_{50} (μm)	40	25

Note. Further details of these products are available under the producer's web site (http://www.sasoltechdata.com/alumina_group.asp).

[a]The test substances are high-purity aluminas from Sasol.

Test design. The test materials were examined sequentially in two independent but similarly performed 4-week inhalation studies. Each study was conducted as follows: at the end of the acclimatization period rats were randomly assigned to four exposure groups. Each group consisted of 54 male rats. All rats per group were exposed in directed-flow nose-only inhalation chambers to targeted concentrations of 0 (control), 0.4, 3, and 28 mg/m^3 for 4 weeks (6 h/day on 5 days/week). The studies differed in that they attempted to minimize (AlOOH-40 nm/MMAD-0.6 μm) or maximize (AlOOH-10 nm/MMAD-1.7 μm) the aerodynamic particle size in inhalation chambers. Rats exposed under otherwise identical test conditions to dry, conditioned air served as concurrent control group. After 2 weeks of exposure from days 0–9 an interim sacrifice was made on day 10. Postexposure sacrifices commenced on target days 35, 56, and 113. Rats were sacrificed one day after the last exposure. On each sacrifice 12 rats per group were used (six for lavage and histopathology, six for toxicokinetic examinations in various compartments).

Clinical observations were systematically performed on individual rats before and after exposure. Body weights were recorded twice weekly on Mondays and Fridays during the exposure period and once weekly thereafter. The focus of study was to examine and associate dose-response and time-course changes of inflammatory end points in lungs by bronchoalveolar lavage (BAL) with dispositional pulmonary end points. Likewise, the translocation of particulates into extrapulmonary organs (see "Disposition of Aluminum") was included in this analysis.

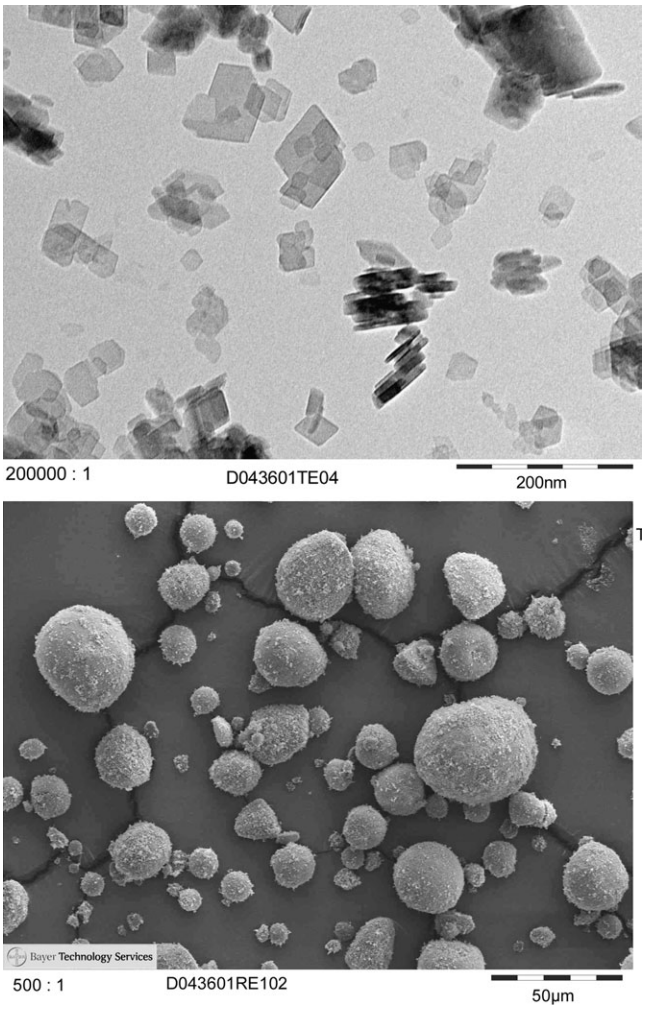

FIG. 1. Aluminum oxyhydroxide primary nanocrystals of AlOOH-40 nm (Pural), (upper panel). Typical agglomerated micronsized particles of bulk substance after dispersion (lower panel).

Exposure technique and atmosphere generation. The powders were dispersed into inhalation chambers using a Wright-Dust-Feeder (BGI, Inc., Waltham, MA). AlOOH-10 nm had a low dustiness. Therefore, it was micronized to enhance the dustiness of the bulk material. For micronization a Retsch Centrifugal Ball Mill S100 (http://www.retsch.com/dltmp/www/08b12c73a43c42cdfd57224c6296b12/brochure _ball_mills_en.pdf) was used. Grinding jars contained agate balls (100 × 10 mm balls). The micronization lasted 10 min at 400 revolutions/min. Heat stress to the test article was minimized by this procedure. The mass ground per batch did not exceed 50 gram. Prior to entering the nose-only inhalation chamber a cyclone and pull/push-dilution system were used to achieve the targeted particle size and concentration. Briefly, pressurized dry, clean air was used for powder dispersion. The flow rate per exposure port was 0.75 l/min. The inhalation chamber used had 80 exposure ports in total. The test atmosphere generation conditions provide an adequate number of air exchanges per hour (> 200 /h, internal chamber volume ≈3.8 l). Under such test conditions steady state is attained within approximately 1 min of exposure. The ratio between the air supplied and exhausted was chosen so that approximately 90% of the supplied air was removed from the chamber as exhaust. The remainder provides adequate dead-space ventilation for the exposure tubes. The test atmosphere can by no means be diluted by bias-air-flows via exposure tubes. The inhalation chamber was operated in a well ventilated chemical fume hood. The exhaust air was purified via cotton-wool and HEPA filters. Details of this modular chamber and its validation have been published in detail elsewhere (Pauluhn, 1994; Pauluhn and Thiel, 2007).

Air flows were monitored and controlled (adjusted) real-time by calibrated mass flow meters (Hastings HFC-C Mass Flow Controllers, Teledyne Hastings-Raydist, Hampton, VA or TYLAN FC-280 S mass flow controllers, TYLAN General, Torrance, CA). The proper performance of the mass flow controllers was measured using a digital precision flow-meter calibration device (Bios DryCal Defender 510; http://www. smglink.com/bios/drycal_defender/drycal_defender.html). Humidity sensors were calibrated using saturated salt solutions according to Greenspan (1977) in a two-point calibration at 33% ($MgCl_2$) and at 75% (NaCl) relative humidity. The absence of larger particles (cut-off of cyclone ≈10 µm) and high flow rates in the vicinity of the sampling ports make it possible to disregard potential anisokinetic sampling errors, thus ensuring a representative sampling even with different sampling probe orifice diameters and flow rates. The tolerance limits for the radius of the probe orifice were calculated using published formulas (ACGIH, 1978; Willeke and Baron, 1993).

Control of the inhalation chamber and management of all physical inhalation chamber data, including the current calibration data, were performed using a computerized and validated data acquisition and control system. This system continuously monitors, controls, and/or records the inhalation chamber parameters: supply and exhaust air, sampling activities (mass flow controlled supply and exhaust air flows, sampling air flow rates from filter analyses, real-time aerosol monitoring (Microdust Pro, Casella, or TEOM 1400a, Thermo Fisher Scientific, East Greenbush, NY), temperature und humidity (FTF11 sensors, Elka Elektronik, Lüdenscheid, Germany), and ambient pressure (Vacuubrand CVC24).

Exposure atmosphere characterization. In addition to continuous real-time monitoring of atmospheres, breathing zone concentrations were characterized by filter analyses (glass fiber filters, Sartorius, Göttingen, Germany). The sampling rate was 4 l/min in all groups. For each filter analysis the sampled volume was ≈1200, 300, and 80 l at 0.4, 3, and 28 mg/m^3, respectively. Particle size analyses were made using a low-pressure critical orifice Berner-Type AERAS stainless steel 11-stage cascade impactor with effective cut-off diameters from 0.016 to 16 µm (HAUKE, Gmunden, Austria). Silicon-coated aluminum foil served as collection medium of particles. The mass median aerodynamic diameter (MMAD) and the geometric standard deviation (GSD) were calculated as described previously (Pauluhn, 2005a). Flow rates were controlled by a critical orifice at 4.7 l/min. The sampling duration was 320, 90, and 10 min at 0.4, 3, and 28 mg/m^3, respectively. Due to the extensive sampling duration required for cascade impactor analyses, preference was given to measurements using a TSI-Laser Velocimeter APS 3321 (TSI Inc., St. Paul, MN, USA). This device detects particles in the range of 0.5–20 µm. The sampling duration was 2 min in all groups at different dilutions (Diluter TSI Model 3302).

Bronchoalveolar lavage. Rats assigned to BAL analyses were anesthetized with sodium pentobarbital (Narcoren; 120 mg/kg bw, intraperitoneal injection). After complete exsanguination by heart puncture, the excised wet lungs were lavaged via a tracheal cannula with two volumes of 5-ml of physiological saline (at 37°C) and four lavage cycles in total. Pooled BAL was centrifuged at 200 × g for 10 min. at < 10°C (Sigma 4K15C-centrifuge). The cell pellet was re-suspended in PBS-BSA (Dulbecco's phosphate buffered saline with Ca^{2+} and Mg^{2+} containing 0.1% bovine serum albumin; Sigma, Deisenhofen, Germany) and then centrifuged (2×10^5 per cytospot) onto slides using a cytocentrifuge (Shandon Cytospin 4, Life Science International, Frankfurt, Germany). Air-dried slides were fixed with a mixture of methanol:acetone, stained according to Pappenheim, and differentiated by light microscopy (300 cells were counted/cytospot). Cell counts were determined in triplicates after 1:1000 dilution using a CASY cell counter + analyzer (Innovatis, Reutlingen, Germany). In the supernatant the following end points were determined: total cell count, lactate dehydrogenase (LDH), protein, γ-glutamyltransferase (γ-GT), β-N-acetylglucosaminidase (β-NAG), and cytodifferentiation of BAL cells. Protein, γ-GT, and β−NAG were determined according to Layne (1957), IFCC (2002), Maruhn (1976),

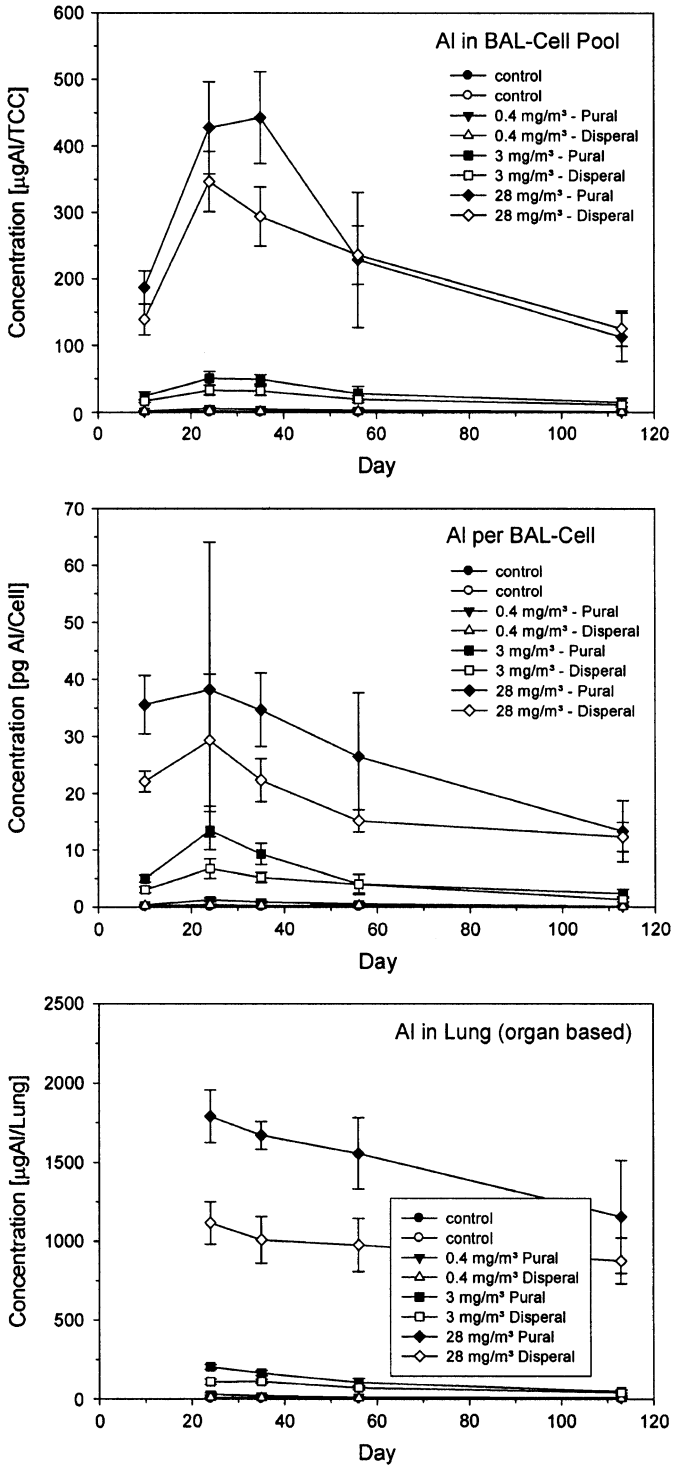

FIG. 2. Time-course and concentration-response analyses of aluminum in lavaged lungs, BAL cells (dose per cell), and total BAL cells (cellular dose multiplied by total cell count) of rats exposed for 4 weeks (6 h/day, 5 days/week) to either pural (AlOOH-40 nm/MMAD-0.6 µm) or disperal (AlOOH-10 nm/MMAD-1.7 µm). Data points represent the mean ± SD of six male rats examined at midterm of the study period (day 10) and on postexposure days 1, 12, 33, 91.

respectively. The remaining parameters were determined using commercially available reagents. Cytodifferentiated cells were expressed as percentage (of 300 counted cells) and as absolute cell counts. Further methodological have been published elsewhere (Pauluhn, 2002).

Histopathology and organ weights. After complete exsanguination of anesthetized rats (Narcoren; 120 mg/kg bw, intraperitoneal injection) the excised wet lungs and hilar lymph nodes (denoted lung-associated lymph nodes, LALNs) were weighed. Lungs were inflated at a pressure of approximately 20 cm H_2O with 10% neutral-buffered formalin, and fixed similarly by immersion. Histopathology was conducted of all 5 lung lobes, including bronchi, LALNs from the hilar region. The examination included sections of the ethmoid turbinates, nerve axon transition to the brain and the bulbus olfactorius. The head with nasal cavities was decalcified (citrate-formic acid) at room temperature for 3 weeks and then, similar to all other sections, embedded with paraplast. Slides were stained with hematoxylin and eosin. Lungs were additionally counterstained with Sirius red for the diagnosis of collagen.

Disposition of aluminum. Biological specimens (urine, brain, right lung lobes, BAL cells, LALNs, kidneys, and liver) were collected after exsanguination at each sacrifice for the determination of aluminum (Al) as marker of exposure (the Al content of AlOOH was ≈43%, see Table 1). All data refer to mass of Al per organ and were converted to the particle mass concentrations of AlOOH by multiplication with 2.3 (100/43). Urine was collected over night on days 4, 11, 18, and 25 and concentrations of aluminum were normalized to creatinine. Organ aliquots were digested and converted to acid-soluble inorganic salts in a mixture of acids (e.g., nitric acid, hydrochloric acid, sulfuric acid, perchloric acid, and/or hydrogen peroxide). This conversion took place in sealed reaction vessels in a temperature range from 130°C to 300°C at 200 bar in a microwave-heated autoclave (Ultraclave MLS). After cooling, solubilized organs were diluted with deionized water.

For all analyses blank solutions and a standard solution of aluminum were used (Al 99.999%; 2% aqueous solution of HNO_3 with a standard concentration of 1000 ± 3 µg Al/ml; CAT-No. 10001-1, High-Purity Standards, Charleston, SC or ICP-Standard aluminum at the same concentration, CAT-No. 03812 from Bernd Kraft GmbH, Duisburg, Germany). The PerkinElmer AAnalyst 700 high-performance atomic absorption (AA) spectrometer with WinLab 32 AA software features was used for analysis of Al. The AA is an automated motorized atomizer exchange that allows switching between flame and graphite furnace AA by a simple software command. The graphite mode was used for determinations. The instrument was equipped with a high performance burner system and TotalFlow gas controls for flame AA and a Heated Graphite Atomizer graphite furnace with deuterium background corrector. The graphite furnace system includes True Temperature Control and pyro tubes, providing full Stabilized Temperature Platform Furnace conditions for almost interference-free trace metal analysis.

Statistical analysis. For simulation of the exposure-related accumulation of particles in the lung the following relationship was assumed: $dc/dt = a(1 - kt)$, where k is the first-order elimination constant empirically determined during the 3-month postexposure period and a is the daily increment of particle dose deposited in the alveoli (for details see Table 3). During exposure days, a fraction of the dose increment was added to each of the arrays, and the total accumulated lung dose was then calculated by the equation shown above over the entire exposure period by superposition of the arrays. A Fortran computer code was used for calculations. BAL and organ weight data were compared by a one-way ANOVA and a Tukey-Kramer post hoc test. The criterion for statistical significance was set at $p < 0.05$. Asterisks in figures and tables denote statistically significant differences to the concurrent air control group, $*p < 0.05$ and $**p < 0.01$.

RESULTS

Exposure Atmosphere Characterization

Analysis of aerosol particle size distributions from the breathing zone samples obtained with a critical orifice cascade

TABLE 2
Generation and Characterization of Chamber Aerosol Atmospheres (Means of Representative Exposure Period, ± SD where Applicable)

	AlOOH-40 nm/MMAD-0.6 μm				AlOOH-10 nm/MMAD-1.7 μm			
Target concentration (mg/m^3)	0	0.4	3.0	28.0	0	0.4	3.0	28.0
Exposure atmosphere characterization								
Gravimetric concentration (mg/m^3)	—	0.4 ± 0.11 ($n = 17$)	3.3 ± 0.55 ($n = 60$)	28.7 ± 3.2 ($n = 60$)	—	0.4 ± 0.06 ($n = 16$)	3.1 ± 0.32 ($n = 60$)	28.3 ± 3.3 ($n = 60$)
Total chamber air flow (l/min)	60	60	60	60	60	60	60	60
Total exhaust air flow (l/min)	54	54	54	54	54	54	54	54
Temperature-chamber (°C)	21 ± 0.2	22 ± 0.3	21 ± 0.2	22 ± 0.3	21 ± 0.2	22 ± 0.3	21 ± 0.2	22 ± 0.2
Relative humidity-chamber (%)[a]	5 ± 0	5 ± 0	5 ± 0	5.1 ± 0.2	5 ± 0	5 ± 0	5 ± 0	5.1 ± 0.1
Particle size analysis by Berner critical orifice cascade impactor								
MMAD (μm)	—	0.59 ± 0.1 ($n = 4$)	0.57 ± 0.05 ($n = 12$)	0.63 ± 0.05 ($n = 12$)	—	1.75 ± 0.19 ($n = 4$)	1.65 ± 0.12 ($n = 12$)	1.68 ± 0.16 ($n = 12$)
GSD	—	2.47 ± 0.3	2.63 ± 0.14	2.56 ± 0.18	—	2.71 ± 0.2	2.79 ± 0.14	2.72 ± 0.23
Respirability (% mass < 3 μm)	—	96.6	95.7	95.2	—	70.9	72.2	72.0
Mass concentration (mg/m^3)		0.38 ± 0.02	3.5 ± 0.34	29.6 ± 4.8		0.34 ± 0.06	3.0 ± 0.31	30.0 ± 2.49
Particle size analysis by laser velocimeter TSI APS 3321								
MMAD (μm)	—	0.88 ± 0.08 ($n = 4$)	0.87 ± 0.06 ($n = 4$)	0.84 ± 0.06 ($n = 4$)	—	2.20 ± 0.11 ($n = 4$)	2.32 ± 0.03 ($n = 4$)	2.45 ± 0.18 ($n = 4$)
NMAD (μm)	—	0.72 ± 0.08	0.70 ± 0.03	0.66 ± 0.02	—	0.81 ± 0.04	0.87 ± 0.02	0.84 ± 0.02
GSD	—	1.60 ± 0.02	1.81 ± 0.10	2.07 ± 0.4	—	1.84 ± 0.02	1.89 ± 0.04	1.81 ± 0.08
Number concentration (particles/cm^3)	—	112.1 ± 112	4404 ± 1518	39,525 ± 8653	—	249.8 ± 112	2895 ± 246	24,075 ± 7904

Note. NMAD, number median aerodynamic diameter; GSD, geometric standard deviation; —, not applicable.

[a]Lower confidence range of humidity sensor 5%. Values represent means ± SD. Off-line sampling activities (n reflects the number of filter and particle analyses per group) which were adequately spaced during the course of the 4-week exposure period. Temperature and humidity values were continuously recorded on-line and means and standard deviations were from daily means. Air flow rates were electronically controlled and adjusted to the set flow rate.

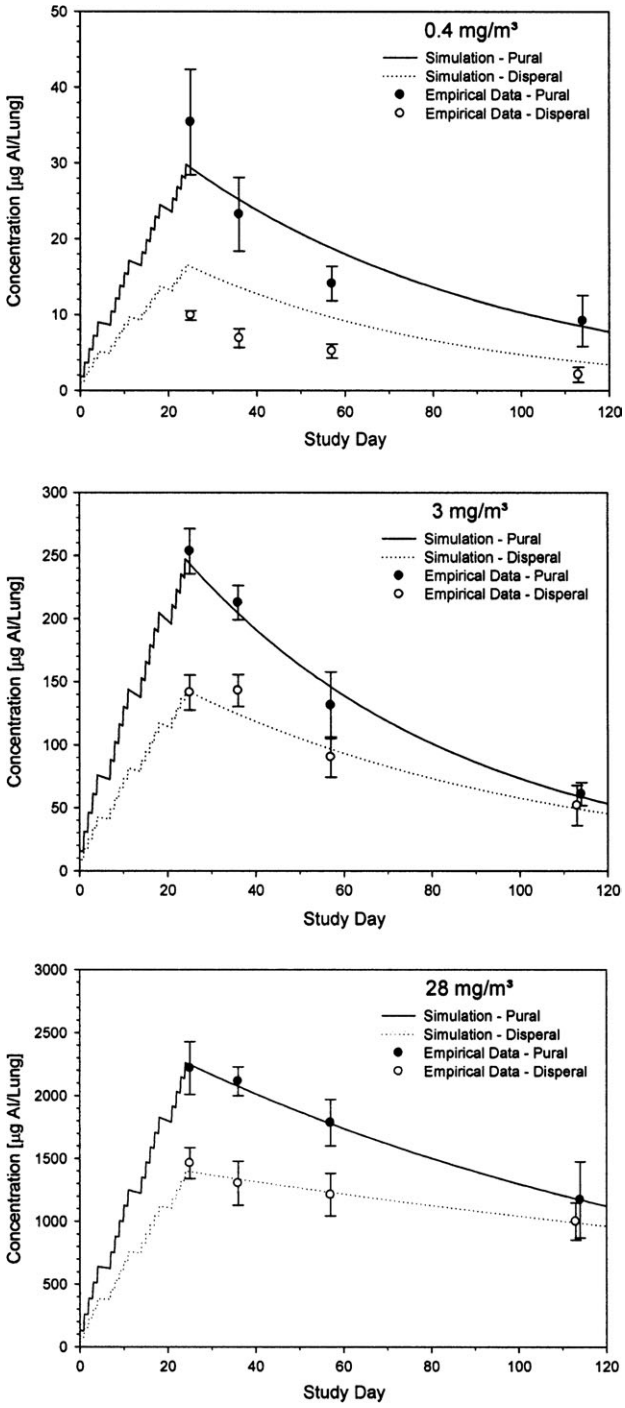

FIG. 3. Comparison of simulated and empirical concentrations of aluminum in lungs of rats exposed for 4 weeks (6 h/day, 5 days/week) to either pural (AlOOH-40 nm/MMAD-0.6 μm) or disperal (AlOOH-10 nm/MMAD-1.7 μm). Calculations were based on the parameters detailed in Table 3. Empirical data points represent mean ± SD of the total aluminum burden of lungs (aluminum in lung tissue and total BAL cells combined). Six male rats were examined on postexposure days 1, 12, 33, 91 (study days 24, 35, 56, 113) as detailed in Figure 2.

impactor and TSI APS 3321 laser velocimeter, despite the entirely different physical principles, delivered essentially similar results (Table 2). In the AlOOH-40 nm/MMAD-0.6 μm exposure groups, the average MMAD obtained by cascade impactor and TSI APS 3321 analyses was ≈0.6 μm (GSD 2.6) and ≈0.9 μm (GSD 1.6–2.1), respectively. In the AlOOH-10 nm/MMAD-1.7 μm exposure groups, the respective MMADs were ≈1.7 μm (GSD 2.7) and ≈2.3 μm (GSD 1.8). The total mass concentrations from cascade impactor analyses were essentially similar to filter analyses (Table 2). This demonstrates that anisokinetic sampling errors did not occur to any appreciable extent. The slightly higher MMAD provided by the laser velocimeter appears to be due, *inter alia*, to the limited detection of particles less than 0.5 μm.

Clinical Observations and Body Weights

The 4-week exposure to both aluminum oxyhydroxides was tolerated without any substance-induced signs or mortality and concentration-dependent changes in body weights. At 0, 0.4, 3, and 28 mg/m^3 AlOOH-40 nm/MMAD-0.6 μm body weights (means ± SD) at the commencement of the exposure period (day 0, 54 rats per group) were 233 ± 10.3 g, 232 ± 10.2 g, 228 ± 11.6 g, and 230 ± 10.9 g and at the end of the 4-week exposure period (day 25, 42 rats per group) 286 ± 16.8 g, 275 ± 18.6 g, 276 ± 18.5 g, and 279 ± 16.1 g. In the AlOOH-10 nm/MMAD-1.7 μm study the respective body weights were as follows: 235 ± 9.9 g, 234 ± 9.6 g, 234 ± 11.2 g, and 235 ± 10.9 g and at the end of the 4-week exposure period 296 ± 19.0 g, 284 ± 16.0 g, 286 ± 22.5 g, and 286 ± 19.2 g.

Pulmonary and Extrapulmonary Disposition

Aluminum (Al) served as tracer metal for the analysis of the pulmonary and extrapulmonary disposition of particles. Although this method cannot unequivocally differentiate between dissolved tissue-bound and particle-associated tracer metal, the extremely low solubility of calcined aluminum oxyhydroxide justifies the approach chosen. Tracer determinations in the brain and kidneys were restricted to the control and high-level exposure groups (end of exposure period and 2 weeks postexposure) while determinations in the liver included all postexposure interim sacrifices. Statistically significant differences in Al concentrations in the control and exposure groups did not occur in any organ and at time point (data not shown). The urinary levels of Al measured toward the end of each exposure week revealed in all groups aluminum concentrations in the range of 5 μg Al/mmol creatinine without any conclusive time- or concentration-dependent increased excretion of Al (data not shown).

The 4-week nose-only exposure of rats to concentrations of 0.4, 3, and 28 mg/m^3 resulted in concentrations of Al in lungs fairly proportional to the respective cumulative exposure dose when accounting for the differences in alveolar deposition (Figs. 2 and 3; Table 3). For estimation of alveolar deposition (respirability) calculations referred to mass-based cascade

impactor analyses. Based on the kinetic parameters summarized in Table 3 and accounting for the different respirabilities of particles of AlOOH-40 nm/MMAD-0.6 μm and AlOOH-10 nm/MMAD-1.7 μm in inhalation chambers, the simulated time-course of the cumulative pulmonary dose of Al matched the empirical data reasonably well at 3 and 28 mg/m^3 for both aluminas. However, at 0.4 mg/m^3 simulated data from AlOOH-10 nm/MMAD-1.7 μm were slightly over-predicted, whilst the respective data from AlOOH-40 nm/MMAD-0.6 μm matched the prediction (Fig. 3).Relative to AlOOH-40 nm, the elimination half-time of AlOOH-10 nm was over-proportionally increased at 28 mg/m^3 (Table 3).

The compartmental kinetics of elimination of Al in lungs (lavaged) and in BAL cells differed in a cumulative-dose dependent manner (Figs. 2 and 4). For both aluminas the elimination of Al via the BAL-cell pool (mainly alveolar macrophages) was faster than that from lung tissue (Fig. 1, Table 3). Although the compartmental elimination half-times were in the range or below 60 days at 0.4 and 3 mg/m^3 for both aluminas, a precipitous prolongation of elimination occurred especially in the lung following exposure to 28 mg/m^3 (Fig. 3, Table 3). With regard to particle mass, the prolonged elimination was observed at ≈2 mg particle mass/g lung but was minimal or absent equal or below fourfold lower cumulative lung doses. The compartmentalization of Al in lung tissue, total BAL cells, and LALNs is compared in Figure 4. Despite the wide spacing of exposure concentrations and differences in particle size of the inhaled aluminas, the relative percentages of particle burdens in BAL cells relative to the total pulmonary burdens were quite similar (Fig. 4). The lung (lavaged) and BAL-cell contents were highly correlated (Fig. 5). Also the translocation of tracer into LALNs appears to be highly dependent on the accumulated pulmonary dose. Although this translocation was minimal at 0.4 and 3 mg/m^3 for both aluminas, differences were clearly apparent at 28 mg/m^3. The translocation of Al into LALNs of AlOOH-10 nm/MMAD-1.7 μm-exposed rats was less as compared with AlOOH-40 nm/MMAD-0.6 μm-exposed rats (Figs. 4 and 6).

Bronchoalveolar Lavage

Significant differences of end points measured in BAL following exposure to 0.4 and 3 mg/m^3 of AlOOH-40 nm/MMAD-0.6 μm or AlOOH-10 nm/MMAD-1.7 μm did not occur at any time point. The occurrence of significant differences to the time-matched control was restricted to the 28 mg/m^3 exposure groups. In rats sacrificed toward the end of the 4-week exposure period, changes were characterized by increased LDH, β-NAG, protein, γ-GT, total cell counts, and PMNs (Figs. 7 and 8). Following 2-week of exposure to 28 mg/m^3 (day 10, interim sacrifice), only minimal changes were observed. These were restricted to significantly increased γ-GT, protein (AlOOH-10 nm/MMAD-1.7 μm only), and PMNs. With the exception of increased PMNs (AlOOH-40 nm/MMAD-0.6 μm and AlOOH-10 nm/MMAD-1.7 μm) and LDH (AlOOH-10 nm/MMAD-1.7 μm only) the end points measured regressed to the level of the time-matched control at the end of the 3-month postexposure period. In regard to the relative inflammogenic potencies of AlOOH-40 nm/MMAD-0.6 μm and AlOOH-10 nm/MMAD-1.7 μm at 28 mg/m^3, clear differences were not apparent. However, with regard to the increased influx of PMNs, exposure to AlOOH-10 nm/MMAD-1.7 μm caused a slightly more pronounced and sustained effect (Fig. 9).

Lung and LALN Weights, Histopathology

Wet lung weights were indistinguishable between groups at the interim sacrifice (day 10). Lung weights were maximally increased after the 4-week exposure period at 28 mg/m^3 (Fig. 10). Also the LALN weights were significantly increased at 28 mg/m^3 after 4 weeks but not 2 weeks. AlOOH-40 nm/MMAD-0.6 μm and AlOOH-10 nm/MMAD-1.7 μm were indistinguishable at 0.4 and 3 mg/m^3, whereas at 28 mg/m^3 slightly different time-course patterns of changes in lung and LALN weights were observed (Fig. 11).

Histopathology findings attributable to AlOOH poorly soluble particles were only found in rats exposed at 28 mg/m^3. At the end of the 4-week exposure period, these were characterized by particles in alveoli and alveolar macrophages, some of them displayed an enlarged and foamy appearance. In the bronchioloalveolar region a slight hypercellularity (increased epithelial cells, inflammatory cells, focal septal thickening; all changes were graded very slight to minimal) occurred. In Sirius red stained sections, focal septal collagen depositions existed. LALNs showed a slight lymphoid activation associated with an increased accumulation of epitheloid cells with extended postexposure duration. Changes in the pulmonary region did neither progress nor regress during the 3-month postexposure period. Differences between AlOOH-40 nm/MMAD-0.6 μm and AlOOH-10 nm/MMAD-1.7 μm were not found. The examination of the *bulbus olfactorius* by light microscopy, including the ethmoid nasal passages, did not provide evidence of particle translocation or specific local alterations (data not shown).

DISCUSSION

With the increased emergence of engineered nanomaterials some new and unusual risks have been postulated, but there is relatively little consistent information on how these risks can be identified and assessed in a scientifically rationalized as well as internationally harmonized manner. With regard to pulmonary biopersistence, fate and toxicity, common denominators of dose and response across the diverse subset of particles are discussed controversially (Maynard, 2007; Oberdörster *et al.*,

TABLE 3
Estimated Deposited Alveolar Fractions and Dose of Inhaled Aerosols of AlOOH-40 nm/MMAD-0.6 μm and AlOOH-10 nm/MMAD-1.7 μm

	AlOOH-40 nm/MMAD-0.6 μm			AlOOH-10 nm/MMAD-1.7 μm		
	Concentration (mg/m^3)					
	0.4	3	28	0.4	3	28
Deposited alveolar fraction[a]	0.105	0.108	0.103	0.063	0.067	0.065
Dose per day (μg Al/rat)[b]	1.85	15.7	130	1.06	8.7	77.2
Lung tissue—$t_{1/2}$ (days)[c]	56	43	144	42	60	295
BAL-cell—$t_{1/2}$ (days)[c]	25	37	59	33	38	79
Lung tissue and total BAL-cell content combined—$t_{1/2}$ (days)[d]	50	43	94	42	58	177

Note. Kinetic parameters were calculated based on tissue aluminum concentrations assuming a first-order elimination kinetics of particles. Tissue concentrations were examined following a 4-week inhalation period using a 6 h/day, 5 days/week exposure regimen on postexposure days 1, 12, 33, 91.

[a]Dosimetric adjustment with regard to particle size (based on cascade impactor analyses, see Table 2) was made using the Multiple-Path Particle Dosimetry Model (MPPD2) (Anjilvel and Asgharian, 1995; RIVM, 2002).

[b]The aluminas examined had an aluminum content as shown in Table 1 (39–44%). For the conversion of Al to AlOOH a common factor of 2.3 (100/43) was used.

[c]Based on log-transformed analysis of data depicted in Figure 2.

[d]The fate of inhaled particles (see Fig. 2) was calculated based on elimination rate constants ($k = \ln(2)/t_{1/2}$ [days^{-1}]) of the lung, that is, rate constants of lung tissue (lavaged) and total BAL cells were combined. Simulations were based using a respiratory minute volume of 1 l/min/kg-rat. This respiratory minute volume has been determined under conditions similar to this study (Pauluhn and Thiel, 2007).

1992, 2005, 2007; Stoeger *et al*., 2007; Wittmaack, 2007). To effectively scale pulmonary response data across experimental systems and different particle types requires an understanding of dose-response relationships. In regard to AlOOH, this aspect has been dealt with elsewhere (Pauluhn, in press-a). Opposite to repeated exposure particle inhalation studies, the use of alternative bolus techniques using high bolus doses, often together with unusual vehicle systems to make bolus instillations of high doses of insoluble, hydrophobic material possible, have shown that systemic translocation of particles may occur. However, the related localized inflammatory response and the associated deterioration of the septal barrier function causing such an increased accessibility of particles to the LALNs and/or systemic circulation have received relatively little attention (Pauluhn, in press-b).

The objective of study was to assess lung toxicity of two AlOOH bracketing a size range of primary particles from ≈10 nm (AlOOH-10 nm/MMAD-1.7 μm) to ≈40 nm (AlOOH-40 nm/MMAD-0.6 μm) using a subacute 4-week inhalation rat-bioassay followed by a 3-month postexposure period. Poorly soluble particles have long elimination half-times in the pulmonary system; especially under overloading conditions (see Table 3). The selection of exposure concentrations took into account results from a previous subchronic 13-week inhalation study with ultrafine TiO_2 (Bermudez *et al*., 2004). Exposure duration adjusted, the intermediate and high cumulative exposure doses used in this study were in the same range as used for TiO_2 (13-week exposure to 2 and 10 mg TiO_2/m^3 is deemed to be dosimetrically equivalent to 6 and 30 mg AlOOH/m^3 after 4-week exposure). Following exposure to TiO_2, pulmonary toxicity was considered to be lung overload related which was also reflected by increased translocation of particles from the lung to the lung-associated lymph nodes and changes in inflammatory end points in BAL (total protein, LDH, and neutrophils). The elimination half-time for alveolar clearance in the non-overloading state (rats) has been reported to be in the range of 50–65 days (Donaldson *et al*., 2008; Stöber and McClellan, 1997). Therefore, although experimentally not expedient and convenient, a 3-month postexposure period is considered to be minimal to evaluate and compare retention-related differences in the toxicokinetics and toxicodynamics of inhaled (nano)particles of low solubility.

Nanoparticles may enter the blood stream, either directly via the lung (after disintegration of inhaled agglomerated particles) or perhaps also via the lymphatic system. However, the fate of nanoparticles within the lung and from the lung into the blood is imperfectly known and needs further study (DEFRA, 2007). Accordingly, the toxicodynamic end points measured in this study were complemented by pulmonary and extrapulmonary toxicokinetic data. Uptake of systemically available particles can occur by the reticulo-endothelial system and especially the liver sinusoids (Pauluhn, in press-b). Also excretion via the kidney cannot be ruled out. These organs, including the brain, have been addressed in this study. Further attempts were made to compare toxicodynamic findings with the internal dose-related ''partico-kinetics'' and to which extent the target-organ dose and effect parameters depend on the MMAD of agglomerated particles in inhalation chambers.

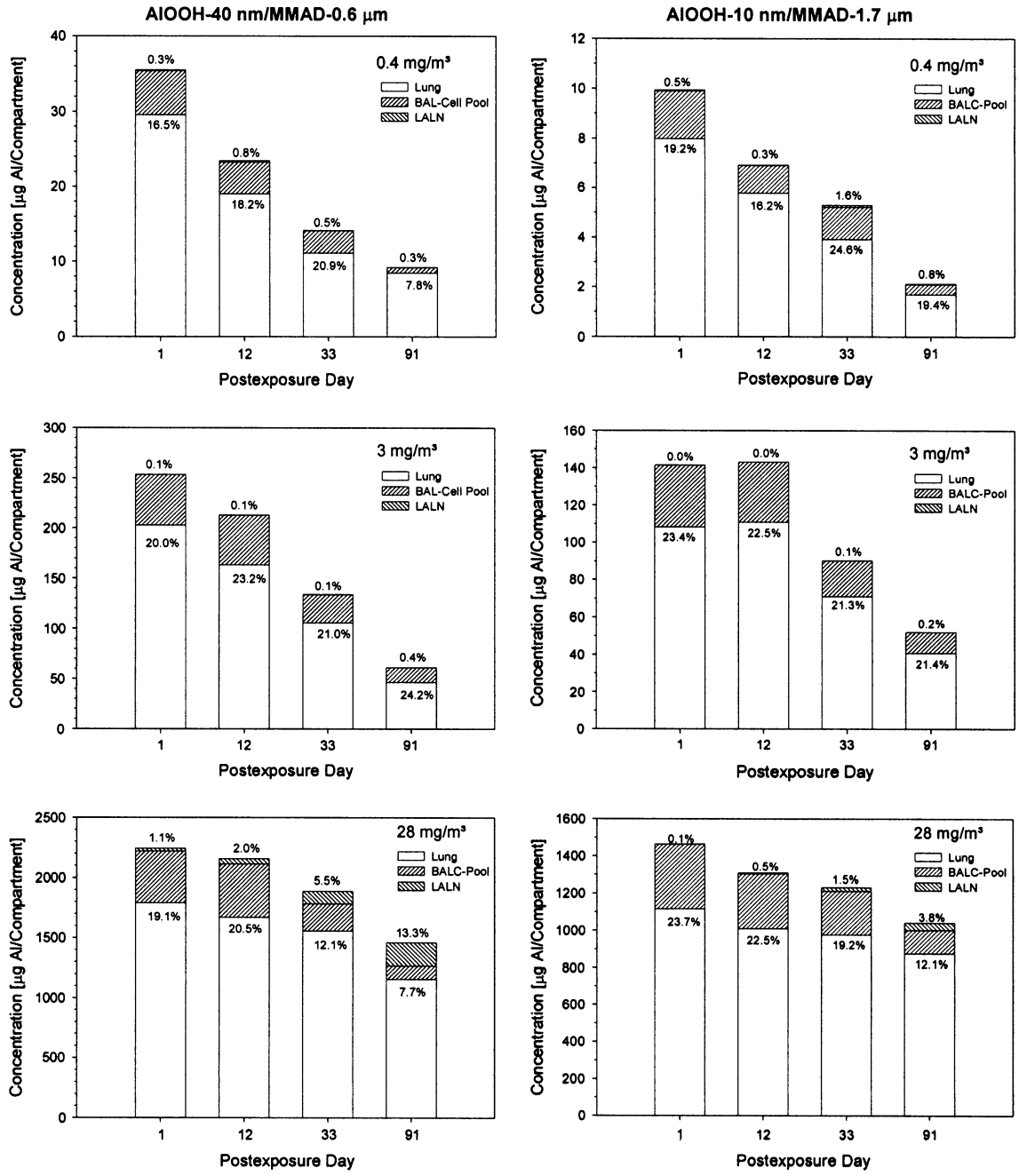

FIG. 4. Compartmental distribution of aluminum in lavaged lungs, total BAL cells, and lung-associated lymph nodes of rats exposed for 4 weeks (6 h/day, 5 days/week) to either pural (AlOOH-40 nm/MMAD-0.6 μm) or disperal (AlOOH-10 nm/MMAD-1.7 μm). Values below and above the hatched areas represent the percentages of Al in the BAL-cell pool and LALNs, respectively; the balance to 100% is concentration in lavaged lungs (not shown). Specimens were collected during a postexposure period of 3 months as detailed in the legend of Figure 3.

This size range of primary particles of the aluminas examined was similar to that of ultrafine anatase/rutile TiO_2 (average particle size ≈25 nm) (Bermudez *et al.*, 2002, 2004; Warheit *et al.*, 2007). The advantage of using AlOOH as a nanosized model structure is that different crystal structures with resultant differences in toxic potency due to dissimilarities in crystal properties (Warheit *et al.*, 2007) are not expected to occur. As already pointed out by Warheit *et al.* (2007), a common finding in inhalation studies is that the MMAD of agglomerated airborne particles is relatively independent on the primary particle size. In studies reported by Bermudez *et al.* (2002, 2004) the TiO_2 primary particle size ranged from 25 nm (ultrafine) to 300 nm (pigment-grade). Yet, the MMADs of particles in inhalation chambers for the two TiO_2 particle-types

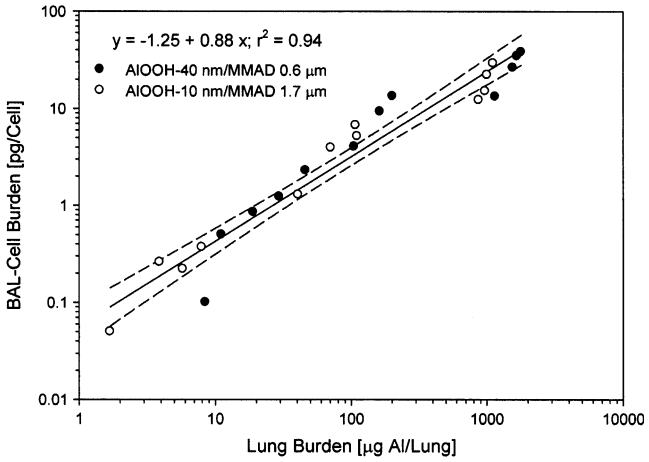

FIG. 5. Correlation of aluminum per BAL-cell and lavaged lung tissue burden. Data points represent means from all measurements (see Fig. 2).

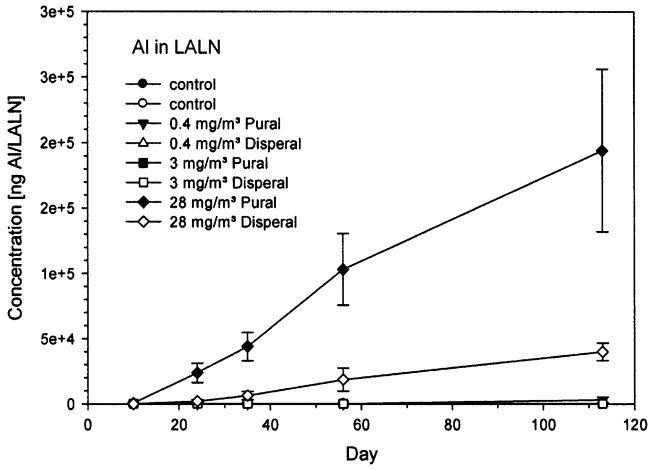

FIG. 6. Time course and concentration dependence of aluminum in lung-associated lymph nodes from rats exposed for 4 weeks (6 h/day, 5 days/week) to either pural (AlOOH-40 nm/MMAD-0.6 µm) or disperal (AlOOH-10 nm/MMAD-1.7 µm). Data points represent the mean ± SD of six male rats examined at midterm of the study period (day 10) and on postexposure days 1, 12, 33, 91.

were similar (MMAD ≈1.4 µm). Despite exposure to agglomerated particles of similar aerodynamic properties, the potency of the ultrafine TiO_2 to cause inflammation and cytotoxicity in subchronically exposed rats was approximately five times greater compared to the pulmonary effects of the inhaled pigment-grade TiO_2 particles (Warheit *et al.*, 2007).

The MMAD of agglomerated particle in inhalation chambers of several aluminas in the primary particle size range 25 ± 15 nm was compared prior to this study (data not shown). This comparison revealed that under the inhalation testing conditions of this study, AlOOH-40 nm/MMAD-0.6 µm produced the smallest MMAD (≈0.6 µm), whereas AlOOH-10 nm/MMAD-1.7 µm produced dust atmospheres with the largest MMAD (≈1.7 µm). Therefore, these two nanosized materials were chosen to study the impact of differences in the agglomerated particle size in inhalation chambers in the absence of potential confounding factors due to changes in crystal properties.

The approach used in this study attempted to add a new facet to the metric of the "internal dose" by quantifying the particle mass load per BAL-cell. This concept has successfully been used earlier for the pulmonary dosimetry of inhaled drugs causing phospholipidosis (Pauluhn, 2005b). The mechanism(s) for nanoparticle uptake are poorly understood, although processes ranging from diffusion-limited uptake to receptor-mediated endocytosis have been reported (Geiser *et al.*, 2005; Kanno *et al.*, 2007). For agglomerated nanoparticles ($\geq$ 0.5 µm), phagocytosis is expected to be a central internalization pathway in macrophages and have been shown to be processed by phagocytotic pathways (Allen and Aderem, 1996; Geiser *et al.*, 2005, 2008; Rabinovitch, 1995). Smaller particles are primarily processed by endocytotic pathways (Takenaka *et al.*, 2006).

The analysis of particle-associated aluminum in BAL cells after the 4-week exposure period in lavaged lungs and BAL cells revealed quite similar relative percentages of particle burden in BAL cells relative to the total pulmonary burden (Fig. 4). The BAL-cell load per se was clearly dependent on the respective exposure concentration and respirability of the inhaled alumina. The high correlation ($r^2 = 0.94$, see Fig. 5) between BAL-cell and lung tissue particle burdens appears to suggest an equilibrium of particles between these two compartments. Alternatively, it can also be hypothesized that most of the particle lung burden (≈80%) is associated with particle-laden resident alveolar macrophages not retrieved by BAL. Inflammatory responses occurred in rats with accumulated doses of approximately 2.2 and 1.5 mg aluminum per lung or 3.9 and 2.7 mg AlOOH-40 nm/MMAD-0.6 µm or AlOOH-10 nm/MMAD-1.7 µm per gram lung (Figs. 2, 3, and 7). At these lung burdens the BAL-cell particle dose was 69×10^{-12} and 92×10^{-12} g AlOOH/BAL-cell for AlOOH-40 nm/MMAD-0.6 µm and AlOOH-10 nm/MMAD-1.7 µm, respectively (Fig. 2). The concentration dependence and time-course changes of aluminum in the lung (Fig. 3) demonstrate a precipitous increase in elimination half-time at this cumulative dose (at 28 mg/m^3) which is consistent with lung-overload. The half-time of poorly soluble particles for alveolar clearance in rats under non-overloading conditions has been reported to be in the range of 50–60 days. Longer elimination half-times occur when the intracellular particle volume exceeds approximately 6% or 60 µm^3 of the phagocytic cell (Morrow, 1988). The reduction in clearance has been attributed, at least in part, to the loss of macrophage mobility at high particle burdens and by volumetric increase of cells by phagocytized particles (Morrow, 1988; Yu *et al.*, 1989). Hence, it appears to be justified to conclude that the pool of particle-laden cells remaining in the lavaged lung equals that cellular pool not be

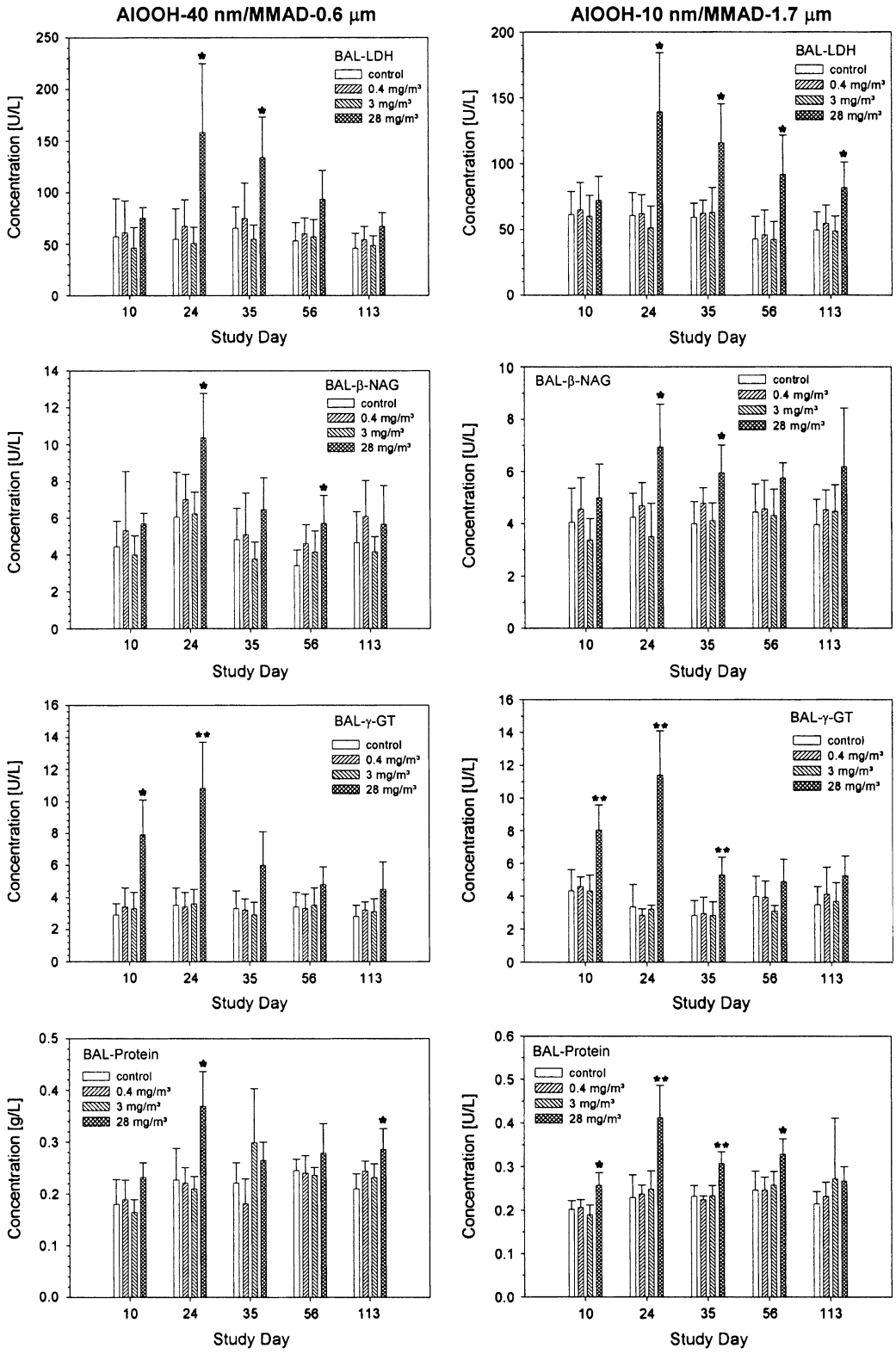

FIG. 7. Comparison of acellular inflammatory end points in BAL fluid. Rats were exposed for 4 weeks (6 h/day, 5 days/week) to either pural (AlOOH-40 nm/MMAD-0.6 μm) or disperal (AlOOH-10 nm/MMAD-1.7 μm). Data points represent the mean ± SD of six male rats examined at midterm of the study period (day 10) and on postexposure days 1, 12, 33, 91 (study days 24, 35, 56, 113). Bars represent mean ± SD. Asterisks denote statistical significance to the time-matched control (*$p < 0.05$, **$p < 0.01$, n = six male rats per group and time point).

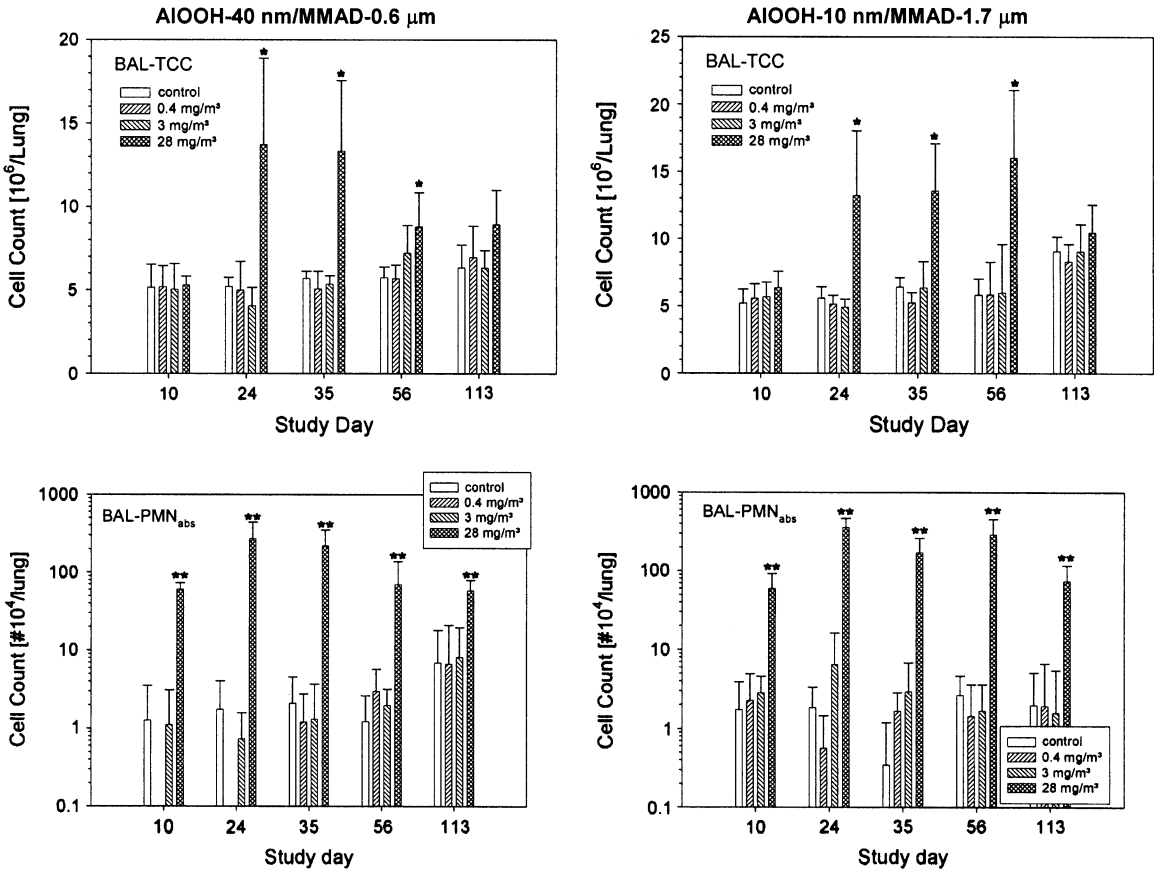

FIG. 8. Comparison of cellular inflammatory end points in BAL. Abbreviations: TCC, total cell count, PMN, neutrophilic granulocytes (absolute counts). For further details see legend of Figure 7.

accessible by lavage. Following exposure to 0.4 mg/m^3 and cumulative lung burdens of 29 and 16 μg Al/lung (67 and 37 μg AlOOH/lung), the kinetic behavior of 40 nm AlOOH-40 nm/MMAD-0.6 μm could be predicted reasonably well (Fig. 3); however, for the 10 nm AlOOH-10 nm the actual retained dose was lower than predicted. It is conceivable that the smaller particles size and larger surface area of 10 nm AlOOH-10 nm/MMAD-1.7 μm facilitates particle dissolution at very low tissue concentrations. The increased clearance half-time of AlOOH-10 nm at overloading lung burdens suggests a greater potential for particle accumulation over extended exposure periods relative to AlOOH-40 nm.

Interestingly, at half the accumulated lung dose (interim sacrifice after 2 weeks of exposure) only minimal pulmonary inflammation occurred (Figs. 9, 11). Translocation of particles to the draining hilar lymph nodes (LALNs) did not occur to any appreciable extent following this exposure period. In turn, to ascertain test article-specific differences in the translocation to the LALNs, a postexposure period of 3 months appears to be required (Fig. 6). Moreover, the translocation of tracer into LALNs appears to be highly dependent on the accumulated pulmonary dose and associated inflammatory response. Although this translocation was absent or minimal at 0.4 and 3 mg/m^3 for both aluminas, differences were clearly apparent at 28 mg/m^3 (Fig. 6).

The determination of aluminum as tracer of exposure to AlOOH did not reveal any evidence of dose- or time-dependent increased Al in the brain, liver, and kidneys. Concentrations of aluminum in urine did also not demonstrate any conclusive time- or dose-dependent changes. These findings support the conclusion that extrapulmonary translocation of aluminum did not occur to any appreciable extent at any exposure level. Of note appears to be that the extent of translocation of AlOOH-40 nm/MMAD-0.6 μm to the LALNs at 28 mg/m^3 was approximately 2 and 6% after 2 and 4 weeks postexposure, respectively, whereas markedly lower concentrations in LALNs were observed following exposure to AlOOH-10 nm/MMAD-1.7 μm (Fig. 4); despite somewhat similar inflammatory responses (Fig. 9) and organ weights (Fig. 11). As already emphasized above, the 3-month postexposure period used is substantially shorter than the particle clearance half-times at 28 mg/m^3 (Table 3). Hence, to better understand the somewhat unclear time-course changes occurring after the 3-month postexposure period (BAL-PMN, Fig. 9; lung and LALN

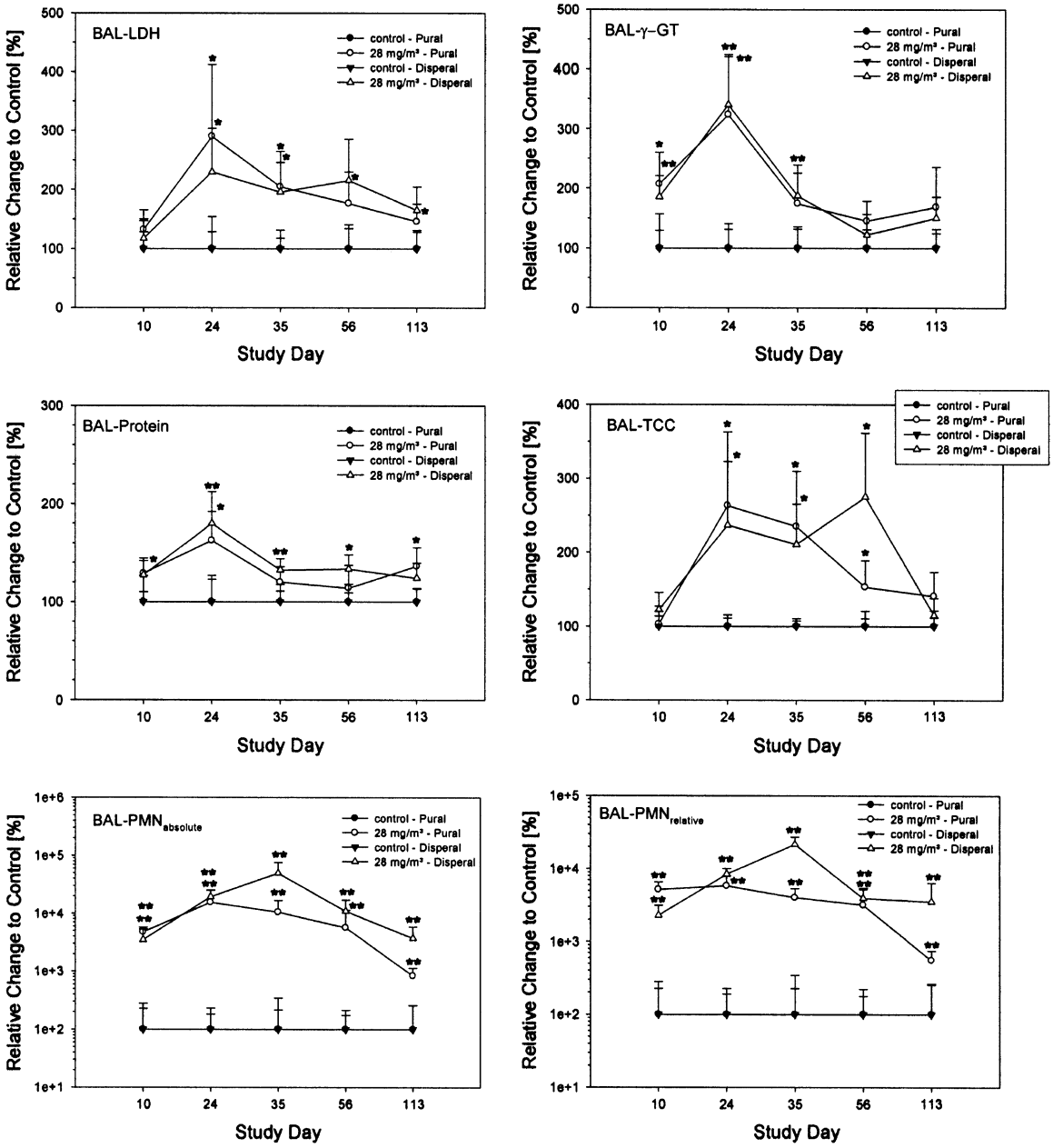

FIG. 9. Comparison of most salient effect parameters in BAL of rats exposed for 4 weeks (6 h/day, 5 days/week) to either pural (AlOOH-40 nm/MMAD-0.6 μm) or disperal (AlOOH-10 nm/MMAD-1.7 μm) at 28 mg/m^3. Data points represent the mean ± SD of data calculated relative to the time-matched control (=100%) of six male rats per group and time point. For further details see legend of Figure 7.

weights, Fig. 11), yet longer postexposure periods may be useful.

In summary, determination of aluminum in lung tissue provides strong evidence that the cumulative lung exposure dose corresponds well with the mass-based and agglomerated particle size-adjusted external exposure concentration and associated pulmonary inflammatory response. The findings obtained at 28 mg/m^3 with AlOOH after 4 weeks were consistent with those described at 10 mg/m^3 for ultrafine TiO_2 after 13-week exposure by Bermudez *et al*. (2004). Despite high lung burdens, conclusively increased extrapulmonary organ burdens did not occur at any exposure concentration and time point. Although at 0.4 and 3 mg/m^3 increased aluminum could be verified in lung tissue and BAL cells, associated adverse effects were not apparent. Particle-induced pulmonary inflammation was restricted to the high cumulative doses occurring only at 28 mg/m^3 over an exposure period of 4 weeks. In regard to particle lung burdens, the results of this

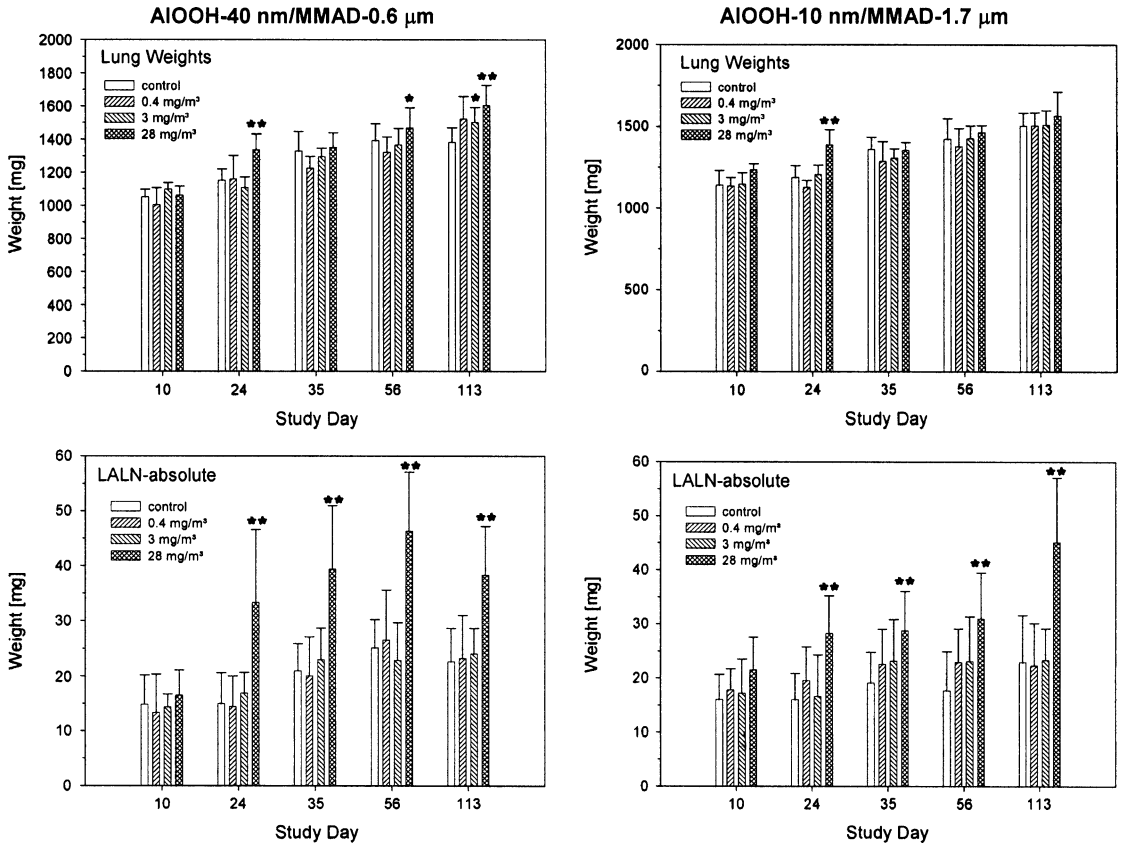

FIG. 10. Lung and LALN weights from rats exposed for 4 weeks (6 h/day, 5 days/week) to either pural (AlOOH-40 nm/MMAD-0.6 μm) or disperal (AlOOH-10 nm/MMAD-1.7 μm). Data points represent the mean ± SD of six male rats per group and time point. For further details see legend of Figure 7.

study are consistent with other studies, using various particulates, showing that at lung burdens of ≈1 mg/g lung or greater there is prolonged retention of particles (Morrow, 1992). Of note is that particle lung burdens more than twice as high (Al concentrations in lungs following exposure to 28 mg/m^3 x 100/43 × 1/1.2; see Table 1 for Al content in AlOOH, Fig. 3 for concentrations of Al in lungs, and Fig. 10 for lung weights), evoked markedly less pronounced responses (if any) after 2 weeks exposure (see day 10, Figs. 9 and 11) when compared with the 4-week exposure period. Hence, these

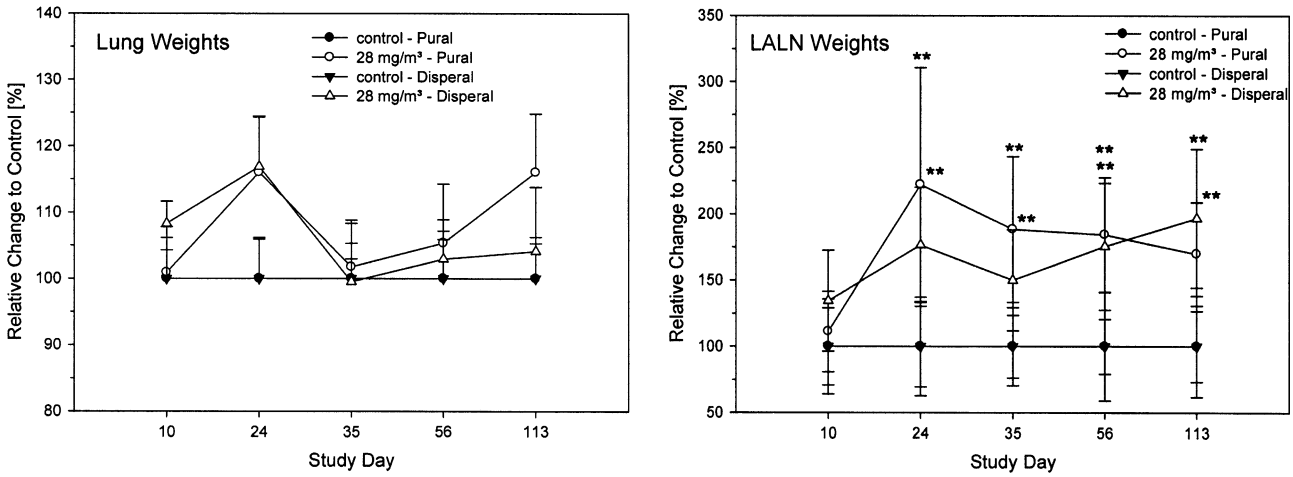

FIG. 11. Comparison of lung and LALN weights of rats exposed for 4 weeks (6 h/day, 5 days/week) to either pural (AlOOH-40 nm/MMAD-0.6 μm) or disperal (AlOOH-10 nm/MMAD-1.7 μm) at 28 mg/m^3. Data points represent the mean ± SD of data calculated relative to the time-matched control (=100%) of six male rats per group and time point. For further details see legend of Figure 7.

results demonstrate that a 4 week exposure protocol with a minimal postexposure period of 3 months appears to be necessary to adequately reveal and characterize the potential hazards of poorly soluble (nano)particles. At identical particle exposure concentrations, lung burdens were substantially higher when the MMAD was ≈0.6 μm as compared with ≈1.7 μm. Therefore, if technically feasible, inhalation studies with an MMAD less than 1 μm should be targeted to maximize the retained pulmonary dose. Overall, it is concluded that the pulmonary toxicity of nanosized, agglomerated AlOOH particles appears to be determined by the size of agglomerated particles while their fate is more dependent on the primary particle size. In regard to the toxicokinetics, the outcome is highly contingent upon the total lung burden and especially whether overloading and non-overloading conditions had been attained. These conclusions are coherent with published evidence (ILSI, 2000).

FUNDING

German Federal Ministry of Education and Research-NanoCare Project.

ACKNOWLEDGMENTS

The author thanks Dr Loof, for determinations in lung lavage, Dr Schweer (Currenta) for Aluminum determinations in tissues, and Prof. Dr M. Rosenbruch for histopathology data.

REFERENCES

ACGIH (American Conference of Governmental Industrial Hygienists). (1978). Air Sampling Instruments for Evaluation of Atmospheric Contaminants, 5th ed., ACGIH p. F-6. ACGIH section I: Calibration of Air Sampling Instruments and section F: Aerosol Sampling for Particle Size Analysis.

Allen, L. H., and Aderem, A. (1996). Mechanisms of phagocytosis. *Curr. Opin. Immunol.* **8,** 36–40.

Anjilvel, S., and Asgharian, B. (1995). A multiple-path model of particle deposition in the rat lung. *Fundam. Appl. Toxicol.* **28,** 41–50.

Bermudez, E., Mangum, J. B., Asgharian, B., Wong, B. A., Revery, E. E., Janszen, D. B., Hext, P. M., Warheit, D. B., and Everitt, J. I. (2002). Long-term pulmonary responses of three laboratory rodent species to subchronic inhalation of pigment-grade titanium dioxide particles. *Toxicol. Sci.* **70,** 86–97.

Bermudez, E., Mangum, J. B., Wong, B. A., Asgharian, B., Hext, P. M., Warheit, D. B., and Everitt, J. I. (2004). Pulmonary responses of mice, rats, and hamsters to subchronic inhalation of ultrafine titanium dioxide particles. *Toxicol. Sci.* **77,** 347–357.

DEFRA (Department for Environment, Food and Rural Affairs). (2007). Characterising the potential risks posed by engineered nanoparticles. A second UK Government Research Report. Internet Defra Publication. Available at: www.defra.gov.uk

Directive 86/609/EEC. (1986). Guideline of the Council dated November 24, 1986 on the reconciliation of legal and administrative regulations of the member countries for the protection of animals used for studies and other scientific purposes. *J. Eur. Community Legal Specif.* **29,** 1–28.

Donaldson, K., Aitken, R., Tran, L., Stone, V., Duffin, R., Forrest, G., and Alexander, A. (2006). Carbon nanotubes: A review of their properties in relation to pulmonary toxicity and workplace safety. *Toxicol. Sci.* **92,** 5–22.

Donaldson, K., Borm, P. J. A., Oberdorster, G., Pinkerton, K. E., Stone, V., and Tran, C. L. (2008). Concordance between In vitro and In vivo dosimetry in the proinflammatory effects of low-toxicity, low-solubility particles: The key role of the proximal alveolar region. *Inhal. Toxicol.* **20,** 53–62.

Donaldson, K., and Seaton, A. (2007). The Janus faces of nanoparticles. *J. Nanosci. Nanotechnol.* **7,** 4607–4611.

Duffin, R., Mills, N. L., and Donaldson, K. (2007). Nanoparticles—A thoracic toxicology perspective. *Yonsei Med. J.* **48,** 561–572.

Ferin, J., Oberdorster, G., and Penny, D. (1992). Pulmonary retention of ultrafine and fine particles in rats. *Am. J. Respir. Cell. Mol. Biol.* **6,** 535–542.

Geiser, M., Casaulta, M., Kupferschmid, B., Schulz, H., Semmler-Behnke, M., and Kreyling, W. (2008). The role of macrophages in the clearance of inhaled ultrafine titanium dioxide particles. *Am. J. Respir. Cell. Mol. Biol.* **38,** 371–376.

Geiser, M., Rothen-Rutishauser, B., Kapp, N., Schürch, S., Kreyling, W., Schulz, H., Semmler, M., Im Hof, V., Heyder, J., and Gehr, P. (2005). Ultrafine particles cross cellular membranes by nonphagocytic mechanisms in lungs and in cultured cells. *Environ. Health Perspect.* **113,** 1555–1560.

Greenspan, L. (1977). Humidity fixed points of binary saturated aqueous solutions. *J. Res. Natl. Bureau Standards* **81,** A(1).

IFCC. (2002). IFCC (International Federation of Clinical Chemistry and Laboratory medicine)—Primary reference procedures for the measurement of catalytic activity concentrations of enzymes at 37 °C: Part 6. Reference procedure for the measurement of catalytic concentration of γ-glutamyl-transferase. *Clin. Chem. Lab. Med.* **40,** 734–738.

International Life Science Institute (ILSI). (2000). The relevance of the rat lung response to particle overload for human risk assessment: A workshop consensus Report—ILSI Risk Science Institute Workshop Participants. *Inhal. Toxocol.* **12,** 1–17.

Kanno, S., Furuyama, A., and Hirano, S. (2007). A murine scavenger receptor MARCO recognizes polystyrene particles. *Toxicol. Sci.* **97,** 398–406.

Layne, E. (1957). Spectrophotometric and turbidimetric methods for measuring proteins. II. Protein estimation with the Folin-Ciocalteu reagent. *Methods Enzymol.* **3,** 447– 454.

Maruhn, D. (1976). Rapid colorimetric assay of beta-galactosidase and N-acetyl-beta-glucosaminidase in human urine. *Clin. Chim. Acta* **73,** 453–461.

Maynard, A. D. (2007). Nanotechnology: The next big thing, or much ado about nothing? *Ann. Occup. Hyg.* **51,** 1–12.

Monteiller, C., Tran, L., MacNee, W., Faux, S., Jones, A., Miller, B., and Donaldson, K. (2007). The pro-inflammatory effect of low-toxicity low-solubility particles, nanoparticles and fine particles, on epithelial cells in vitro; the role of surface area. *Occup. Environ. Med.* **64,** 609–615.

Morrow, P. E. (1988). Possible mechanisms to explain dust overloading of the lungs. *Fundam. Appl. Toxicol.* **10,** 369–84.

Morrow, P. E. (1992). Dust overloading in the lungs. *Toxicol. Appl. Toxicol.* **113,** 1–12.

National Institute for Public Health and the Environment (RIVM). (2002). *Multiple path particle dosimetry model (MPPD2 v. 1.0): A model for human and rat airway particle dosimetry*. RIVA Report 650010030. Bilthoven, The Netherlands.

Oberdörster, G., Ferin, J., and Morrow, P. E. (1992). Volumetric loading of alveolar macrophages (AM): A possible basis for diminished AM-mediated particle clearance. *Exp. Lung Res.* **18,** 87–104.

Oberdörster, G., Oberdörster, E., and Oberdörster, J. (2005). Nanotoxicology: An emerging discipline evolving from studies of ultrafine particles. *Environ. Health Perspect.* **113,** 823–839.

Oberdörster, G., Oberdörster, E., and Oberdörster, J. (2007). Concepts of nanoparticle dose metric and response metric. *Environ. Health Perspect.* **115,** A290.

Pauluhn, J. (1994). Validation of an improved nose-only exposure system for rodents. *J. Appl. Toxicol.* **14,** 55–62.

Pauluhn, J. (2002). Short-term inhalation toxicity of polyisocyanate aerosols in rats: Comparative assessment of irritant-threshold concentrations by bronchoalveolar lavage. *Inhal. Toxicol.* **14,** 287–301.

Pauluhn, J. (2005a). Retrospective analysis of acute inhalation toxicity studies: Comparison of actual concentrations obtained by filter and cascade impactor analyses. *Regul. Toxicol. Pharmacol.* **42,** 236–244.

Pauluhn, J. (2005b). Inhaled cationic amphiphilic drug-induced pulmonary phospholipidosis in rats and dogs: Time-course and dose-response of biomarkers of exposure and effect. *Toxicology* **207,** 59–72.

Pauluhn, J., and Thiel, A. (2007). A simple approach to validation of directed-flow nose-only inhalation chambers. *J. Appl. Toxicol.* **27,** 160–167.

Pauluhn, J. Retrospective analysis of 4-week inhalation studies in rats with focus on fate and pulmonary toxicity of two nanosized aluminum oxyhydroxides (boehmite) and pigment-grade iron oxide (magnetite): The key metric of dose is particle mass and not particle surface area. *Toxicology.* (in press-a).

Pauluhn, J. Comparative pulmonary response to inhaled nanostructures: Considerations on test design and end points. *Inhal. Toxicol.* (in press-b).

Rabinovitch, M. (1995). Professional and non-professional phagocytes: An introduction. *Trends Cell Biol.* **5,** 85–87.

Stern, S. T., and McNeil, S. E. (2008). Nanotechnology safety concerns revisited. *Toxicol. Sci.* **101,** 4–21.

Stöber, W., and McClellan, R. O. (1997). Pulmonary retention and clearance of inhaled biopersistent aerosol particles: Data-reducing interpolation models and models of physiologically based systems. A review of recent progress and remaining problems. *Crit. Rev. Toxicol.* **27,** 539–598.

Stoeger, T., Schmid, O., Takenaka, S., and Schulz, H. (2007). Inflammatory response to TiO2 and carbonaceous particles scales best with BET surface area. *Environ. Health Perspect.* **115,** A290–291.

Takenaka, S., Karg, E., Kreyling, W. G., Lentner, B., Möller, W., Behnke-Semmler, M., Jennen, L., Walch, A., Michalke, B., Schramel, P., *et al.* (2006). Distribution pattern of inhaled ultrafine gold particles in the rat lung. *Inhal. Toxicol.* **18,** 733–740.

Warheit, D. B., Brock, W. J., Lee, K. P., Webb, T. R., and Reed, K. L. (2005). Comparative pulmonary toxicity inhalation and instillation studies with different TiO_2 particle formulations: Impact of surface treatment on particle toxicity. *Toxicol. Sci.* **88,** 514–524.

Warheit, D. B., Webb, T. R., Reed, K. L., Frerichs, S., and Sayes, C. M. (2007). Pulmonary toxicity study in rats with three forms of ultrafine.TiO2-particles: Differential responses related to surface properties. *Toxicology* **230,** 90–104.

Warheit, B. D. (2008). How meaningful are the results of nanotoxicology studies in the absence of adequate material characterization? *Toxicol. Sci.* **101,** 183–185.

Willeke, K., and Baron, P. A. (1993). In *Aerosol Measurement—Principles, Techniques, and Applications.* Van Nostrand Reinhold, Yew York.

Wittmaack, K. (2007). Dose and response metrics in nanotoxicology: Wittmaack responds to Oberdörster et al. and Stoeger et al. *Environ. Health Perspect.* **115,** A291.

Yu, C. P., Chen, Y. K., and Morrow, P. E. (1989). An analysis of alveolar macrophage mobility kinetics at dust overloading of the lungs. *Fundam. Appl. Toxicol.* **13,** 452–459.